Impact Tests

21

Luca Goglio

Contents

Abstract

Assessing the mechanical properties of adhesives and the joints strength requires specific tests. Indeed, since polymers are, in general, sensitive to the strain rate they undergo, different phenomena can be induced when a load is applied abruptly. Under such a condition, usually the adhesive tends to react to the deformation with higher stress and lesser ductility, which causes higher resisting loads but lower absorbed energy. This is why the common standard impact tests for adhesives, involving bonded blocks or strips, aim at measuring the energy required to break the bond.

However, since this result is not sufficient to characterize an adhesive, other types of tests have been introduced to obtain a deeper insight. Different types of specimens (samples of bulk adhesive, lap joint, butt joint, double cantilever beam) and test rigs (pendulum, falling weight, hydraulic actuator) have been

L. Goglio (✉)
Department of Mechanical and Aerospace Engineering, Politecnico di Torino, Torino, Italy
e-mail: luca.goglio@polito.it

adopted in many works to measure the properties of interest. The fracture energy, typical of fracture mechanics, requires ad hoc tests and processing to be measured in dynamic conditions. The Split-Hopkinson pressure bar, a special apparatus conceived to test materials at high strain rate, has been also applied with success to adhesives and joints. Also test rigs based on the falling weight schemes have been widely used. A special case is that of conductive adhesives, which are getting into use to replace soldering in electronic packaging: their capability to withstand the impact that a device can undergo in use must be assessed.

This chapter, mainly relying on the results available from the technical literature, presents a survey of various test methods, focusing on the related problems and achievements.

21.1 Introduction

In many of the applications in which adhesives are used, it is likely that they are exposed to loads applied abruptly. A first case is that of a bonded assembly included in a mechanism which, in its service, undergoes discontinuous loading. Examples are mechanisms which undergo intermitting contact, or machineries which exert a crushing action on a material (like mills), or devices conceived to absorb impacts regularly. A second case is that of structures which under normal service are not loaded impulsively but in special conditions (accidents of various types) can be subjected to impacts. This is especially true for automotive applications, in which the crashworthiness is of crucial importance, but it also applies to devices which accidentally can undergo impacts (for instance, due to misuse, fall, etc.). According to the case, the expectations are different: if the impacts are a normal service condition, they must be sustained repeatedly without damage; otherwise, if the impact is an exceptional case, the goal is to minimize its consequences, accepting that a certain level of damage (sometimes high) is unavoidable. It can be remarked that in the former case, the determination of the adhesive performance can be expressed in terms of force or stress, while in the latter case, the typical quantity involved is the absorbed energy.

Two typical issues arise about the behavior of an adhesive subjected to impact. The first one is whether an abrupt loading can cause brittle behavior in a material that under static or quasi-static conditions would not be brittle; this aspect is critical regarding the capability of absorbing energy. The second issue is assessing the influence of the loading rate on the adhesive response, i.e., the sensitivity of the adhesive properties to the strain rate.

It is clear that such issues, all concerning material response, need experimental results to be addressed. For this reason, ad hoc tests have been proposed and developed, also as international standards. The commonest is the block impact test, defined as an American Society for Testing and Materials (ASTM) standard – and subsequently also as European Standard (EN) and International Organization for Standardization (ISO) standard – in which an impact is applied, with a loading scheme similar to that of the Izod pendulum, to a block bonded to a base. Another

popular test, especially in the automotive industry, is the impact wedge peel test, originally developed by Ford and presently also defined as an ISO standard; in this case the bond between two sheet metal strips is broken by a wedge that goes through the joint. These two tests are described in the next two sections of this chapter.

In addition to these standard tests, a considerable amount of research on the impact of adhesives has been carried out and presented by many scientists over the last four decades. A special apparatus, developed for testing materials under high strain rate and applied also to adhesives, is the Hopkinson bar, described in a subsequent section. A selection of other special testing methods and the related modeling are described in a further section.

In many cases, apart from the rupture energy (which can be obtained directly with pendulum-like devices), the measurement carried out in impact testing is the force time history. The typical feature of the latter is its oscillating behavior – posing serious problems when analyzing the curve – which is justified by two arguments. The first explanation is based on the discontinuous nature of crack propagation: when the critical condition is attained, the crack grows, and this relieves the local stresses and makes the system more compliant; thus the load decreases; then, as the impactor advances further, the cycle restarts. The second explanation considers that the specimen receiving the impact starts to vibrate, independently of the damage that can occur. Moreover, the vibrational properties are not necessarily a feature of the specimen alone, since they often depend on the system formed by the specimen and the test rig (which comes into play with its deformability). Unfortunately, in many cases it is very difficult to distinguish one contribution from the other, especially when the recorded time history is the only information available. The operation of smoothing the recorded curve (e.g., by filtering the high-frequency content) implies the risk of losing some useful information; on the other hand, the raw data can be misleading, in the sense that purely dynamic effect can be taken as material properties (e.g., force peaks at breakage). Thus, the evaluation of impact measurements often requires careful judgment, to avoid erroneous interpretation and false results.

It is clearly impossible to recall in a short space all the experiences about impacts tests on adhesives reported in the literature and describe in detail the findings. The objective of the present review is to give general information about what is (and can be) done in this field regarding the experimental arrangements adopted, the types of results obtained, and the behaviors observed. Another broad and detailed state-of-the-art review on adhesives and joints under impact has been very recently presented by Machado et al. (2017). From these reviews, an interested reader could get an address to select the types of experiments and results that fit his/her need. Of course, examining the original literature is always recommended. Among the several contributions appeared in recent times, the special issue of the Int. J. of Adhesion and Adhesives on "Impact phenomena of adhesively bonded joints," Sato and Goglio (2015), can be mentioned.

It can be also remarked that often the cited articles are not exclusively dedicated to experimental works, since they report also the numerical and/or analytical modeling of the specimen behavior. This is due both to the use of the experimental results

to validate the models and to the additional insight given by modeling to understand the stress and strain state during the tests.

21.2 Block Impact Tests

The basic principle on which this test, given by the ASTM D950 standard and by ISO 9653:1998 and EN ISO 9653:2000 as well, relies is to apply an impact loading condition, mainly in shear, by means of a test rig similar to that used for Izod resilience measurement. Figure 1 shows the experimental arrangement. An upper block (usually of steel) is bonded onto another larger block which, in turn, is fixed to the base of the test rig. The first block is struck by a hammer, in a direction parallel (at least at the beginning of the impact) to the bond surface. The energy required to fracture the sample is obtained from that lost by the pendulum, considering a correction for the kinetic energy of the projected parts. The reason for using this type of specimen, quite different from a real joint, is double. First, the block offers a large lateral face, which is easy to hit by means of the hammer. Secondly, the scheme aims at creating a condition of pure and constant shear in the adhesive layer.

A thorough analysis of this case has been carried out by Adams and Harris (1996) who, examining the features of this test, have analyzed in detail the contact conditions between hammer and side of the block. In an ideal situation, the impacting surfaces of the hammer and of the block should be perfectly parallel, giving a uniform load on the block. In practice, a certain degree of misalignment is unavoidable. The authors, by means of finite element analyses, have compared (Fig. 2) the ideal case (I) with the limit cases in which – due to misalignment – the contact occurs at the upper edge of the block (case II) or near to the bond (case III). Their main findings are that, even in case of perfect alignment (Fig. 3, case I), the stresses in the

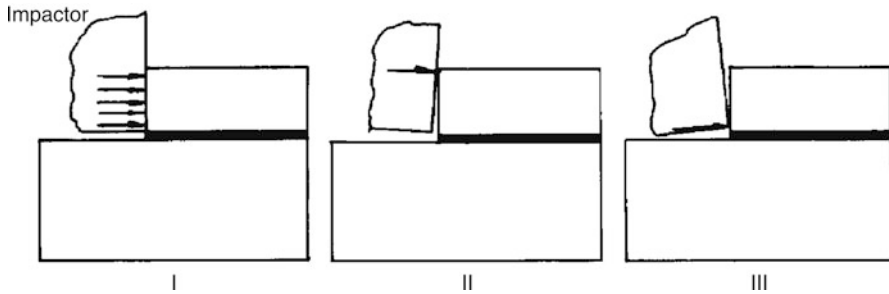**Fig. 1** ASTM block impact test (From Bezemer et al. 1998, copyright Elsevier)
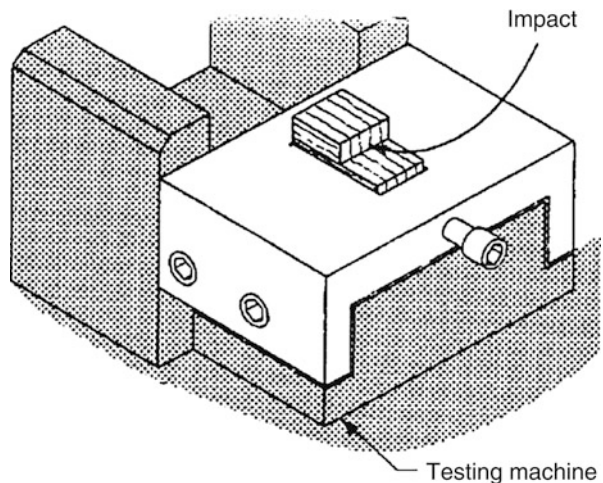
Fig. 2 Possible modes of impact of the pendulum against the block: (**I**) perfectly parallel; (**II**) far from the bond; (**III**) close to the bond (From Adams and Harris 1996, copyright Elsevier)

adhesive are far from being constant: the shear stress peaks near to the bond end at the impacted side; also the peel stress is significant and peaks near to the bond end at the impacted side; then it decreases monotonically assuming negative sign at the opposite bond end. The non-constancy of the shear stress is generated by the "differential straining" mechanism due to the deformability of the block (see ▶ Chap. 24, "Analytical Approach") that emphasizes the stress value at the end of the bond. The peel stress can be primarily regarded as a bending stress caused by the rotation of the impacted block, which – also in this case due to the deformability – is not linearly distributed.

In case of misalignment, the distribution of the shear and peel stress is strongly influenced, as shown in Fig. 3 (cases II and III), due to the changes of moment value and the compressive local deformation of the block (this effect can be regarded as a compression that "irradiates" from the contact point).

If the contact occurs far from the bond (case II), the bending moment is higher, and the peak of peel stress increases, while the local deformation of the block has little influence and the shear stress is not much affected. Conversely, if the contact occurs close to the bond (case III), the combination of low bending moment and compressive local deformation of the block causes a compressive peel stress in the adhesive close to the impacted bond end. At the same time, the local deformation of the block increases the differential straining at the same bond end, which causes a higher peak of shear stress.

Obviously, these features refer to the stress distribution at the beginning of the impact; then the situation evolves depending on the deformations (and damage) that take place. Thus, in global terms, the loading conditions and the strain energy are influenced, depending on the specific case; this aspect is important, since the elastic energy in the steel blocks can be even higher than the rupture energy of the adhesive.

From all these reasons, it comes out clearly that the block impact test is not suitable to give absolute figures about the energy absorption of an adhesive, due to the dependence of the results on the test rig and testing conditions. The only usefulness of the test is that of comparing the behavior of different types of adhesives, but also in this perspective the results must be considered carefully, keeping in mind the importance of the possible misalignments.
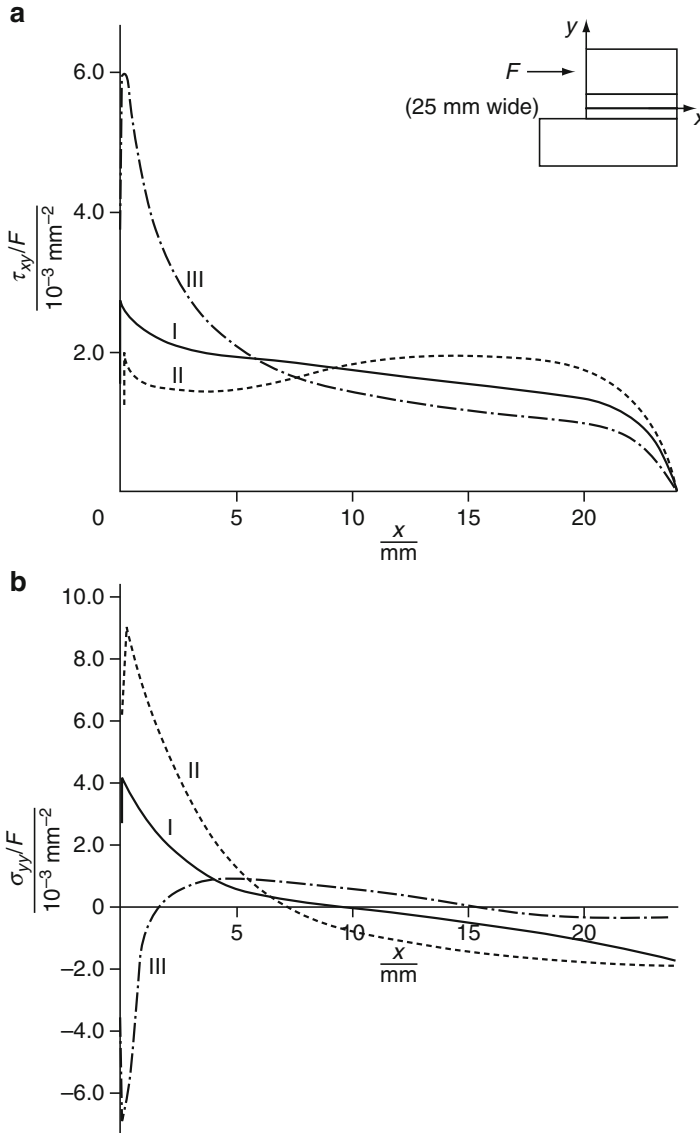
Fig. 3 Stress distribution on the adhesive midplane of the impact block ASTM 250 for different loading cases: (**a**) shear stress; (**b**) peel stress (From Adams and Harris 1996, copyright Elsevier)

An alternative specimen for impact testing of adhesives, aiming at a stress distribution mainly in shear and suitable for a speed higher than that reachable with a pendulum, has been proposed by Bezemer et al. (1998). The specimen in this case is formed by a ring bonded to a coaxial rod; the radial gap defines the desired thickness of adhesive. In the test, the rod is hit axially – and pushed away

from the ring – by a projectile released from a drop tower or launched by an air gun, depending on the speed which is wanted; obviously, also static loading on a standard test machine is possible, especially for the sake of comparison. The contact force between projectile and rod is measured and recorded during the test; hence the displacement can be calculated by integration of the time history, and, in turn, also the energy can be obtained. The authors recognize that, though the motion of the rod with respect to the ring generates a tangential relative displacement, the strains and the stresses are not of pure shear; thus also a considerable normal stress is applied to the adhesive, in spite of the expectation. On the other hand, compared to the block impact, this solution still offers the advantages of a lesser sensitivity to misalignment and broader range of possible loading speed. However, this type of test is not widespread and has not reached the level of a standard.

21.3   Impact Wedge Peel Tests

Another objection against the block impact test is that the adherends involved (blocks) are thick and this does not reflect real applications, in which bonding is usually adopted to join thin parts. From this viewpoint, it appears more realistic to test a bond which joins two metal strips, highly deformable both elastically and plastically. This is just what is done with the "Impact wedge peel test," foreseen by the standards ISO 11343:2003 and EN ISO 11343:2005. The specimen (Fig. 4) is made by two metal strips, formed and bonded together to obtain the shape of a Y. The strips are 90 mm long and 20 mm wide; their thickness can range between 0.6 and 1.7 mm. The bonding length is 30 mm, without any pre-cracking or crack initiator; the not bonded zones form the arms of the Y, which are clamped when the specimen is mounted on the test rig. Even if, to obtain the Y shape, the strips can be formed after bonding, it is recommendable to preform them, to avoid the risk of damaging the adhesive in the forming operation. The specimen is loaded by a wedge which is one side of a rectangular shackle and goes through the bond, thus separating the strips in peeling mode. The pull is applied to the shackle by means of a pendulum
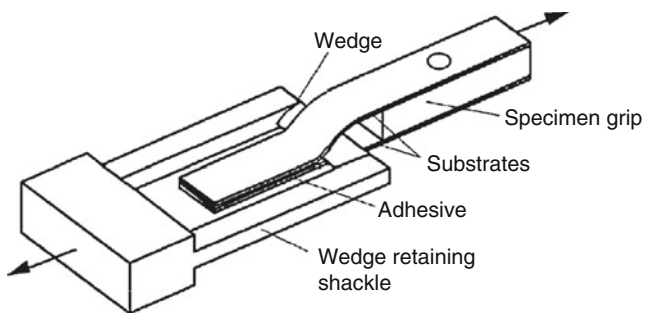

Fig. 4 ISO 11343 wedge impact peel test specimen (From Blackman et al. 2000, copyright Kluwer)

or an actuator, with typical test speeds of 2 or 3 m/s depending on the material of the strips (lower value for steel, higher value for aluminum). During the test, the impact force is measured and recorded for subsequent processing.

A broad study of this test has been carried out by Blackman et al. (2000), who – on the basis of a series of tests carried out on several types of adhesives, at different speeds and temperatures, and using a high-speed hydraulic machine – have analyzed the effect of the specimen geometry and type of crack growth. The onset and the propagation of the rupture have been observed by means of high-speed photography. Furthermore, the authors have reviewed the methods proposed by the standard to extract the results and have applied a finite element model to reproduce the fracture of the specimen.

Two types of crack growth can be observed in this test, stable and unstable. In case of stable growth it has been observed that the crack tip runs ahead the wedge at approximately constant offset; thus the propagation speed is given by the wedge speed. The force time history exhibits initial peaks, due to dynamic effects originated by the sudden contact of the impactor with the specimen, and then a plateau appears and lasts for most of the test. Furthermore, the elevated plastic deformation of the metal strips that takes place involves a considerable amount of strain energy.

In case of unstable growth, typical at low temperature ($-40\ °C$ in these experiments), or with a brittle adhesive, the crack runs rapidly through the whole bond, at a speed much higher than that of the wedge. The force time history after the initial peaks does not exhibit any plateau and oscillates close to zero. After the test, the strips appear almost undeformed, i.e., little plastic deformation takes place, and the measured energy is much lower than in the previous case.

According to the ISO standard, the average cleavage force can be calculated from the time history by considering the data between 25% and 90% of the time interval from the beginning to the end of the curve. The energy is given by the area under the curve between the same end points multiplied by the test speed. The reason for this assumption is to discard the data corresponding to the initial peaks and the "tail" of the curve. Blackman et al. (2000) remark that such procedure works well in case of stable crack growth, but it fails and can lead to false results in case of unstable growth, which does not exhibit any plateau.

An important aspect of the impact wedge peel test is that in case of stable crack growth; part of the energy is spent for deforming the metal strips (this aspect does not affect the unstable crack growth, which, however, is not suitable for the abovementioned reasons). Thus, also with this test, the measurement does not yield a property of the adhesive *in se* but of the assembly formed by adhesive and strips. Another factor that potentially affects the results is the friction between the wedge and the surfaces of the specimen during the fracturing process. However, the finite element simulations performed by Blackman et al. (2000) show that this aspect has minor importance, the leading factor being the adhesive fracture energy G_c. From the knowledge of the latter parameter, which can be measured with a fracture mechanics test such as the double cantilever beam, the time history of the impact wedge test can be reconstructed with finite element modeling.

21.4 Hopkinson Bar Apparatus

In addition to the limitations already mentioned, the two tests described in the previous sections present the further restriction that the strain rate attained in the adhesive cannot be much high, since it usually does not exceed 10^2 s^{-1}. When testing at higher strain rates is needed, the suitable equipment is the so-called Hopkinson bar, which in the last years has become probably the most used by the researchers of the field.

This name is due, historically, to the apparatus used at the beginning of the twentieth century by B. Hopkinson to study the pressure waves generated by explosions or projectiles. In the experiment, the explosion (or the projectile) attained one end of a long and thin bar suspended horizontally, creating a pressure pulse which propagated through the bar until the other end, where a short cylinder of the same diameter of the bar was provisionally attached by means of a grease film or magnetically. This cylinder, called time-piece, was projected by the pulse against a ballistic pendulum which gave the measure of the momentum contained in it; the momentum remained in the bar was measured by observing its oscillation. By varying the length of the time-piece, it was possible to assess the length of the pressure pulse.

The version of the apparatus used nowadays was introduced by Kolsky (1963), who added a second bar, from which the name "Split-Hopkinson pressure bar" comes from; the specimen of material to be tested is inserted between the two bars, as shown schematically in Fig. 5a. The projectile, usually fired by means of a pneumatic gun, impacts the first bar (incident bar), generating the incident pulse which, at the bar/specimen interface, is partially reflected and partially propagates in the specimen. From the specimen, the pulse is transmitted to the second bar
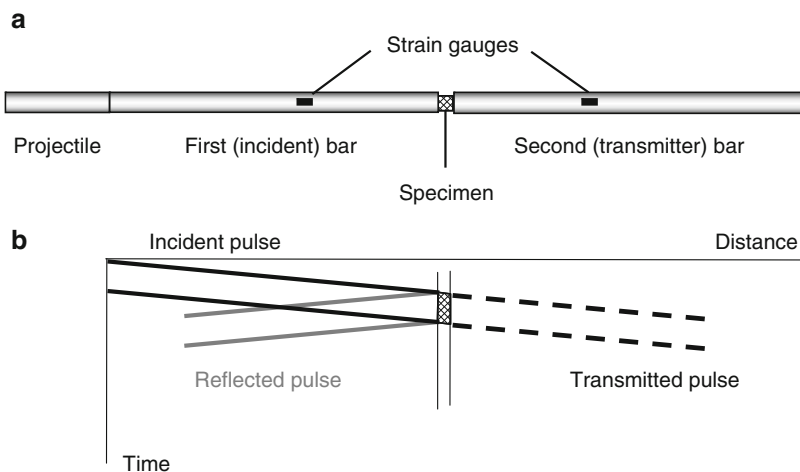

Fig. 5 Schematics of the Split-Hopkinson pressure bar (**a**) and related Lagrangian diagram (**b**)
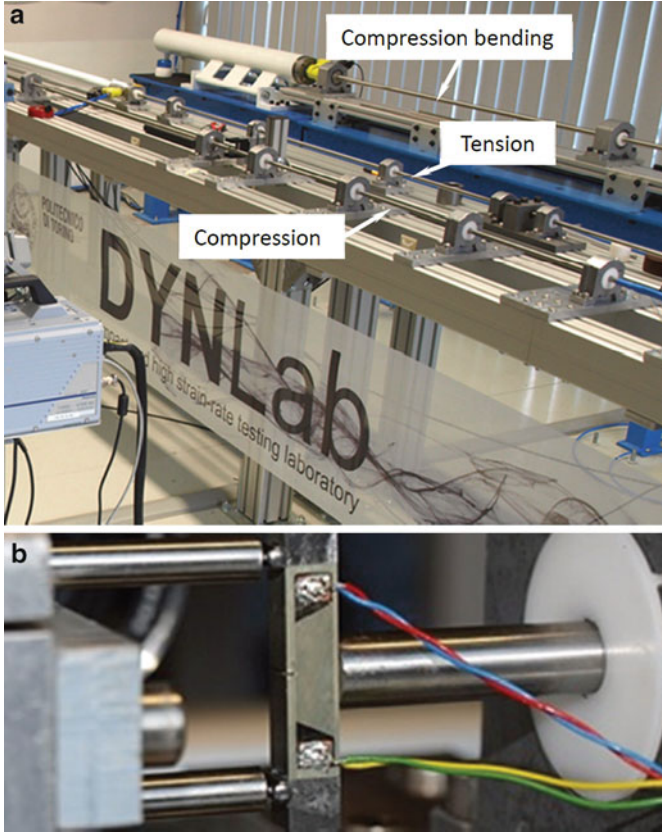
Fig. 6 Split-Hopkinson pressure bar: (**a**) overall view of the rig including three bars for different test conditions; (**b**) detail of the bending fixture (Politecnico di Torino, DYNLAB)

(transmitter bar). The situation is described graphically by the so-called Lagrangian diagram presented in Fig. 5b. A concrete example of Split-Hopkinson pressure bar is shown in Fig. 6. The pulses are measured by means of strain gages placed on both incident and transmitter bar, thus their time history can be stored by means of a transient recorder, usually a digital oscilloscope or an acquisition board. From such measurements the stress (σ), strain (ε), and strain rate ($\dot{\varepsilon}$) in the specimen can be obtained as

$$\sigma(t) = E_0 \frac{A_0}{A} \varepsilon_{\text{tra}}(t) \tag{1}$$

$$\varepsilon(t) = -2 \frac{c_0}{L} \int \varepsilon_{\text{ref}}(t) dt \tag{2}$$

$$\dot{\varepsilon}(t) = -2 \frac{c_0}{L} \varepsilon_{\text{ref}}(t) \tag{3}$$

where, respectively, E_0, A_0, and c_0 are Young's modulus, cross section, and wave velocity of the bar, A and L are the cross section and the length of the specimen, ε_{tra} is the strain pulse transmitted in the second bar, and ε_{ref} is the strain pulse reflected in the first bar. Equations 1, 2, and 3 are based on the assumption that the specimen has reached equilibrium conditions; this requires that its length be smaller than the length of the pulse. Clearly, the measurement cannot be taken directly at the interface; thus the strain gages are placed at a distance from the end of each bar; this is potentially a source of error since the pulses during their travel (from the bar end to the gage) change in shape and assume a delay that must be evaluated.

As far as the adhesives are concerned, the Hopkinson bar has been applied to the characterization of materials and also butt or lap joints. The arrangement described above is suitable for testing in compression (that can be applied by simple contact); in case of tension, the system must be modified, usually by means of a threaded connection. Moreover, it is required to generate a tensile pulse in the bars, and this can be obtained in two ways. The first is to use a reverse loading system, so that the impact of the projectile applies tension to the first bar, as done by Yokoyama (2003) and also (actually to test polymers, but the case would apply also to adhesives) by Chen et al. (2002). The second and more popular solution is to generate, as usually, an initial compressive pulse that travels through both bars; the transmission of this pulse from the first to the second bar is given by a split ring, inserted between them, which prevents the specimen from being loaded in compression (Fig. 7). It is also possible to avoid the use of the split ring if the dimensions of the threaded parts of specimen and bars are accurately manufactured to obtain a precise fit of the ends of the bar (Fig. 8). When the compressive pulse reaches the end of the second bar, it is
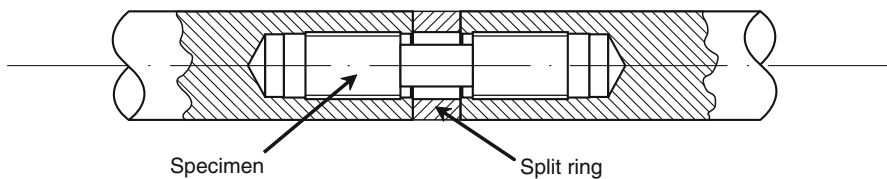

Fig. 7 Use of threaded specimen and split ring to carry out tensile tests with the Hopkinson bar (From Goglio et al. 2008, copyright Elsevier)
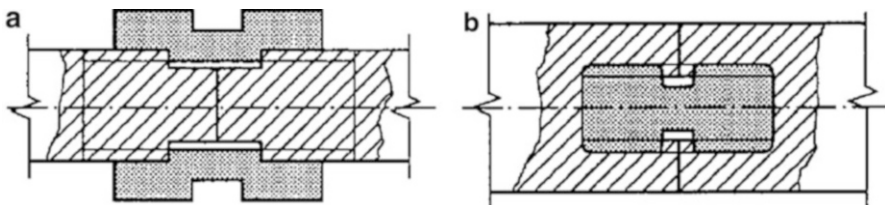

Fig. 8 Use of threaded specimen without split ring to carry out tensile tests with the Hopkinson bar: (**a**) tubular specimen; (**b**) solid specimen (From Bragov and Lomunov 1995, copyright Elsevier)

reflected back as a tensile pulse which stresses the specimen, while the ring gives no contribution under tension.

Several studies based on the Hopkinson bar have been presented by Yokoyama and co-workers. In Yokoyama and Shimizu (1998), the shear strength of pin-and-collar specimens (ASTM D4562) bonded with cyanoacrylate has been studied with the Hopkinson bar and compared to the static case. Both steel and aluminum have been considered as adherend materials. Later, Yokoyama (2003) has tested under tension butt joints made with cyanoacrylate adhesive and two different types of adherends, namely, a bearing steel and a high-strength aluminum alloy. The impact tests have been carried out on a Hopkinson bar; other comparative tests at intermediate and low loading rates have been performed on a standard test machine. The experimental work is supported by a finite element analysis of the stress state in the joint. In both studies, the main findings are that the joint strength, expressed as peak force or stress, increases with the loading rate, while the deformation decreases. There is an optimum value of adhesive thickness (about 35 μm), for which the tensile strength is maximized; furthermore, the strength is influenced by the material of the adherends, steel, or aluminum. In the case of butt joints also the absorbed energy has been evaluated, by integrating the load-deformation curve. It has been noticed that the amount of energy is influenced by the material of the adherends; as in case of steel adherends, it decreases significantly with the loading rate.

Again, Yokoyama et al. (2012a, b) have studied with the Hopkinson bar the response of bulk specimens made of two different structural adhesives (epoxy and methacrylate) tested in compression. A tapered striker has been used to apply a nearly constant strain rate. Both adhesives have shown marked strain rate dependence, and it has been found that a modified Ramberg-Osgood model predicts well the stress-strain curve in loading, but not the strain softening after yielding and the unloading phase.

Recently, Yokoyama and Nakai (2015) have tested brim-and-crown butt joints, fabricated with aluminum alloy or pure titanium and joined by an epoxy. A Hopkinson apparatus modified by adopting a tubular output bar has been used. The experiments have shown that the tensile strength increases significantly with the loading rate and decreases under increasing adhesive thickness, for both adherend types.

Goglio et al. (2008) have tested a bicomponent epoxy under tension and compression, to assess the effect of the strain rate on the strength of this adhesive. Also, in this work both the Hopkinson bar and a hydraulic test machine have been employed, depending on the desired strain rate (from 10^{-3} to 3×10^3 s^{-1}).

Under compression, the stress-strain curve of the adhesive exhibits an initial linear (elastic) rise, then a wide plateau, and again a rise with increasing slope. These features remain the same under any strain rate values, as it can be observed in Fig. 9: increasing the strain rate, the yield stress increases; thus the plateau is shifted upward and starts at larger strain. This observation has led to define a dynamic factor as $k = \sigma_{\text{dynamic}}/\sigma_{\text{static}}$, obtained by the ratio (averaged over the plateau) of the points on the curve at a chosen rate to the points on the static curve. The available data have been used to define prediction formulae for k as a function of the strain rate, based on
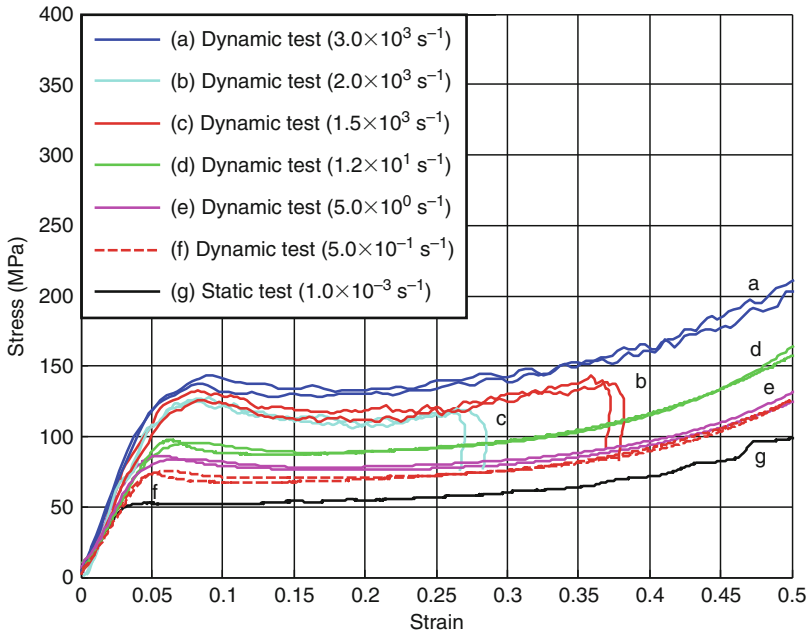
Fig. 9 Dynamic stress-strain curves under compression at different strain rates, case of cold cured adhesive (From Goglio et al. 2008, copyright Elsevier)

a log-log fit as shown in Fig. 10. The two popular models, to account for the strain rate influence, of Cowper-Symonds and Johnson-Cook have been applied to this case. None of them can reproduce the experimental data over the whole range tested (10^{-3}-10^3 s^{-1}); thus they can be conveniently replaced by a poly-linear (in log-log scale) fit in the form $k = A\dot{\varepsilon}^n$, where A and n are coefficients determined over each chosen range. From Fig. 10, it can be also appreciated that the k factor assumes, at the highest strain rate tested, values close to 3; this gives a measure of the elevated sensitivity of the adhesive to the strain rate.

Testing under tension at high strain rate presents particular problems. Apart from the abovementioned modifications to the apparatus required to apply positive stress, the measurement is hindered by the different response of the material. Indeed, the material usually behaves as brittle, and the specimen cracks soon after the stress-strain curve has reached its maximum. The only value that can be obtained is in practice the 0.2% (or other chosen percentage) proof stress. However, this value is also strongly dependent on the strain rate.

There are other specific problems, which affect testing with the Hopkinson bar, that deserve to be mentioned.

One concerns the first part of the stress-strain diagram, corresponding to the elastic behavior and, therefore, useful to evaluate the elastic modulus of the material. This part of the diagram corresponds to a time range of the test in which the equilibrium conditions still have not been achieved in the specimen, since as a
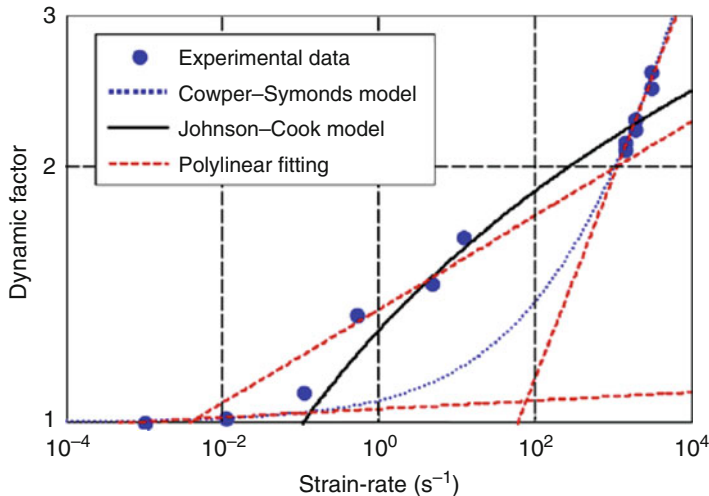
Fig. 10 Dynamic factor k (case of cold cured adhesive): fitting of the experimental values with Cowper-Symonds, Johnson-Cook, and poly-linear models (From Goglio et al. 2008, copyright Elsevier)

practical rule it can be assumed that equilibrium is achieved after the waves have traveled back and forth more than three times along the specimen (Chen et al. 2002). Thus, the values of the elastic modulus can be affected by uncertainty and must be regarded with care.

A general survey – not specifically related to adhesives – of the problems concerning the measurements by means of the Hopkinson bar has been presented by Bragov and Lomunov (1995). Apart from presenting nonconventional applications of the Hopkinson bar (such as dynamic hardness and toughness testing), these authors discuss the problems of signal synchronization and strain rate constancy. The former problem is originated by the difficulty in recognizing the exact beginning of the three measured pulses (incident, reflected, transmitted), which in this paper is corrected by checking that the sum of the incident and reflected pulses equals the transmitted strain pulse. The latter problem is due to the fact that the strain rate, according to Eq. 3, is proportional to the reflected pulse, which decreases as the specimen hardens and its cross section increases during the test. The remedy is to modify the shape of the incident pulse, by means of a tapered projectile or an auxiliary specimen (pulse shaper) placed at the impacted end of the first bar: in this way the incident pulse assumes an increasing amplitude, while the reflected pulse tends to be constant.

Zhao and Gary (1996), presenting a study related to the measurement of small strains with the Hopkinson bar, have considered two important sources of error. The first is the dispersion (related to the difference between phase and group velocities of the waves), which the authors correct with a numerical procedure. The second is the determination of the time delay between the signals, for which an iterative procedure

is proposed. These authors also propose an identification technique to treat the data corresponding to the initial transient of the measurement, when the equilibrium in the specimen is not yet attained.

In a general perspective, not solely related to testing of adhesives, the problem of the dispersion has been considered by Tyas and Watson (2001). They have proposed to correct the measurement by means of two factors, termed M_1 and M_2, one relating measured surface strain to average strain over the cross section and the other relating average axial strain to average axial stress (dynamic elastic modulus).

Another source of error is the effect of the nonuniform distribution of stress and strain over the cross section, related to radial inertia. This problem, considered again in general case by Forrestal et al. (2007), becomes important when the diameter of the bar is large and, therefore, the wave is no longer mono-dimensional. The corrections which are proposed are based on the theoretical solution for the wave propagation.

Sen et al. (2011) have carried out tests on single-lap joints of different overlap lengths; they have found that the (apparent) strength expressed as average stress decreases by increasing the overlap – in accordance to what is found also under static loading – and that the edges of the adhesive are subjected to the maximum strain. An important remark about this type of measurements is that, as stated previously, in Hopkinson bar testing, the stresses should be uniform throughout the length of the sample, which is more difficult to achieve in case of lap joints.

Similarly, Challita et al. (2011) have carried out quasi-static, intermediate, and high strain rate tests (the latter on a Hopkinson bar) on double-lap joints, using compression-shear and tensile-shear specimens. It has been found that the shear strength increases for increasing strain rate until 10^3 s^{-1} then decreases. Correction coefficients based on the previous work Challita and Othman (2010) have been used to estimate the maximum stress, accounting for the nonuniform distribution.

Testing with the Hopkinson bar has been applied also to nonconventional cases, to assess the material response in special conditions. For instance, Martinez et al. (1998) have studied the behavior of a confined adhesive, i.e., when it cannot freely expand laterally under compression. The interest for such case is related to the use of an adhesive to join, in an armored panel, the front ceramic layer to the metal backing plate. To this aim, the adhesive specimen in the Hopkinson bar tests has been surrounded by a confinement tube. The study, carried out on several types of adhesives, has evidenced an optimum value of the adhesive thickness in the armor, in order to ensure enough strength to contain the ceramic fragments and the minimum reflection of the pressure wave. A work by Adamvalli and Parameswaran (2008) has studied the influence of the temperature on the strength of single-lap joints, bonded with an epoxy adhesive, tested at different loading rates (Fig. 11). It has been found that, on the one hand, at the highest loading rate tested (4.7 MPa/μs), the strength is more than three times the corresponding static value; on the other hand, an increase of temperature from 25 °C to 100 °C reduces by 35% the strength.

Ravi Sankar et al. (2015) have used a Hopkinson bar to test lap joints with split-cylinder geometry, made with similar or dissimilar metals (steel, aluminum) joined by an epoxy. The results, supported by finite element modeling to assess the stress
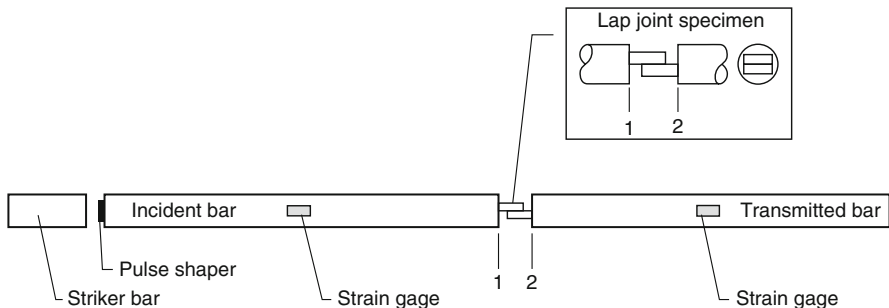
Fig. 11 Setup of the Hopkinson bar for testing lap joints at high temperature (From Adamvalli and Parameswaran 2008, copyright Elsevier)

distribution, indicate that the strength is dictated by the less stiff adherend. A further interpretation by these authors is that the strength measured using the Hopkinson bar represents the volume averaged shear stress in the adhesive layer, as stated by Challita and Othman (2010).

The method of the Hopkinson bar testing has also been applied to specimen types other than cylinders or lap joints.

Sato and Ikegami (1999) have measured the dynamic strength of an epoxy adhesive by testing butt joints of tubes subjected to shear and normal stress. Their equipment (Fig. 12) include a Hopkinson bar suspended vertically and loaded at the upper end by hydraulic actuators which apply, before the beginning of the test, a torsional and a tensile preload. Nearby the lower end, the bar is clamped by a mechanism that can be released rapidly. The specimen is formed by an upper short tube (load input tube), screwed at its upper end to the Hopkinson bar, and a long lower tube (load output tube), instrumented with strain gages. When the clamp is released, the elastic energy accumulated in the bar creates the waves that travel from one tube to the other, thus loading the adhesive layer. The reason for an elevated length of the output tube is to avoid that the back reflection of the waves at its lower end could interfere with the useful signals. The result is a chart, of the type shown in Fig. 13, reporting the failure conditions under different combinations of peel and shear stress. Also, cases of failure under static loading are reported in the diagram, for comparison with the dynamic case; it is evident that the stress values under impact are approximately double than the static ones. The authors have also tried to interpolate the experimental points with the popular Tresca and von Mises failure criteria, but the best fit (solid lines in the figure) is given by a polynomial in the form

$$\tau_d'^2 \left(\sigma_d - \sigma_d' \right) + \sigma_d' \tau_d^2 = 0 \qquad (4)$$

where σ_d and τ_d are the applied normal and shear stresses and σ_d' and τ_d' are the strength values measured experimentally. This formula, although not supported by a theoretical background, has also the merit of predicting an increase of the bearable

Fig. 12 Schematic of the modified Hopkinson bar used by Sato and Ikegami (1999) to test butt joints of tubes under tension and torsion
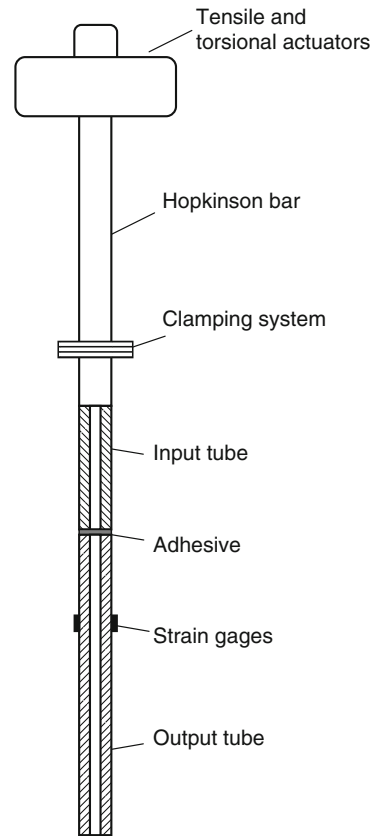
shear stress in case of negative (i.e., compressive) normal stress; this can be noticed by extrapolating to the left the curves in Fig. 13.

An evolution of the Hopkinson bar is the test rig presented by Kihara et al. (2003) to measure the shear strength of adhesive layers (Fig. 14). A prism of hexagonal cross section, screwed between bars 1 and 2, is bonded to a pair of plates which, in turn, are screwed to the additional bars 3. When the pulse, generated from top by the impact of the projectile 0 against bar 1, travels through the prism, it propagates also laterally to the bonds and the plates. The skew slit contained in each plate acts as a reflector which deviates most of the pulse toward bar 3. In addition to the strain gages placed on bar 1 and 2, as usually in the Hopkinson bar scheme, a rosette is applied on each lateral plate to measure the strains in a point close to the adhesive layers. A peculiar phenomenon noticed by the authors is that in case of low incident pulse (in bar 1), the adhesive withstands the shear stress and is fractured by the tensile normal stress generated by the reflection in the plate. Conversely, in case of high incident pulse, it is the shear stress (in combination with compressive stress) that causes the fracture of the adhesive. By means of this apparatus, the authors have
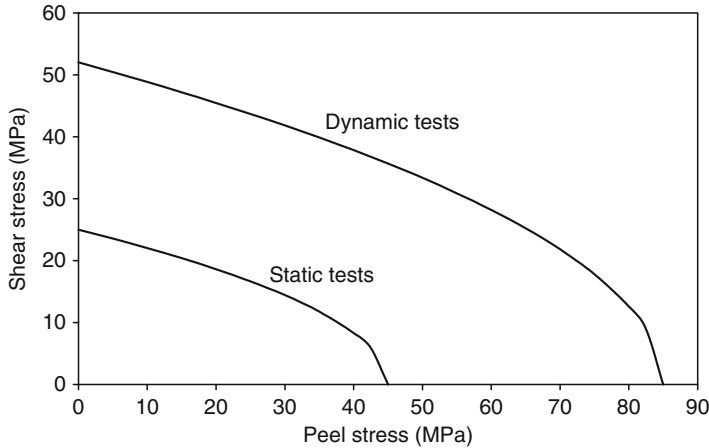
Fig. 13 Limit curves for dynamic and static stress of tubular butt joints subjected to normal and shear stresses based on the results of Sato and Ikegami (1999)

obtained a value of shear strength comparable to that obtainable by cylindrical butt joints subjected to torsion.

Wang and Xu (2006) have performed tensile dynamic tests with the Hopkinson bar on convex-edge joints, shaped in such a way to eliminate the edge singularity in the interface of dissimilar materials, so obtaining a nearly uniform stress distribution and a more correct measurement of the strength. This specimen type is not exactly a bonded joint; however the findings can be useful to design a butt-bonded specimen.

Gilat et al. (2007) have studied the response of two epoxy resins, one untoughened and one toughened, in the strain rate range 10^{-5}–700 1/s, under tensile and torsion loading. Tests at low and medium strain rates have been carried out on a hydraulic (biaxial) machine, those at high strain rates with a tensile or a torsional Hopkinson bar. The latter have been adapted by clamping, respectively, a force or a torque which is then released. A transition from ductile to brittle behavior has been noticed under tension under increasing strain rate; conversely, ductile behavior has been observed under torsional shear at any strain rate.

In a comprehensive work concerning the mechanical properties of the crash-optimized adhesive Betamate 1496 V, May et al. (2015) have used a modified Hopkinson apparatus in which no input bar is foreseen: the striker hits directly the specimen, and the force is measured by a film transducer attached to the end of the output bar. The deformation of the specimen is captured by means an electro-optical system based on a high-speed camera which keeps track of a pair of markers painted on the edges of the specimen.

Very recently, Neumayer et al. (2016) have used a Hopkinson bar to study the impact response of butt- and lap-shear joint specimens, measuring the strain in the adhesive by means of Digital Image Correlation (DIC), achieving a better accuracy than in traditional way. It has been noticed that DIC has given a 12.28 times higher
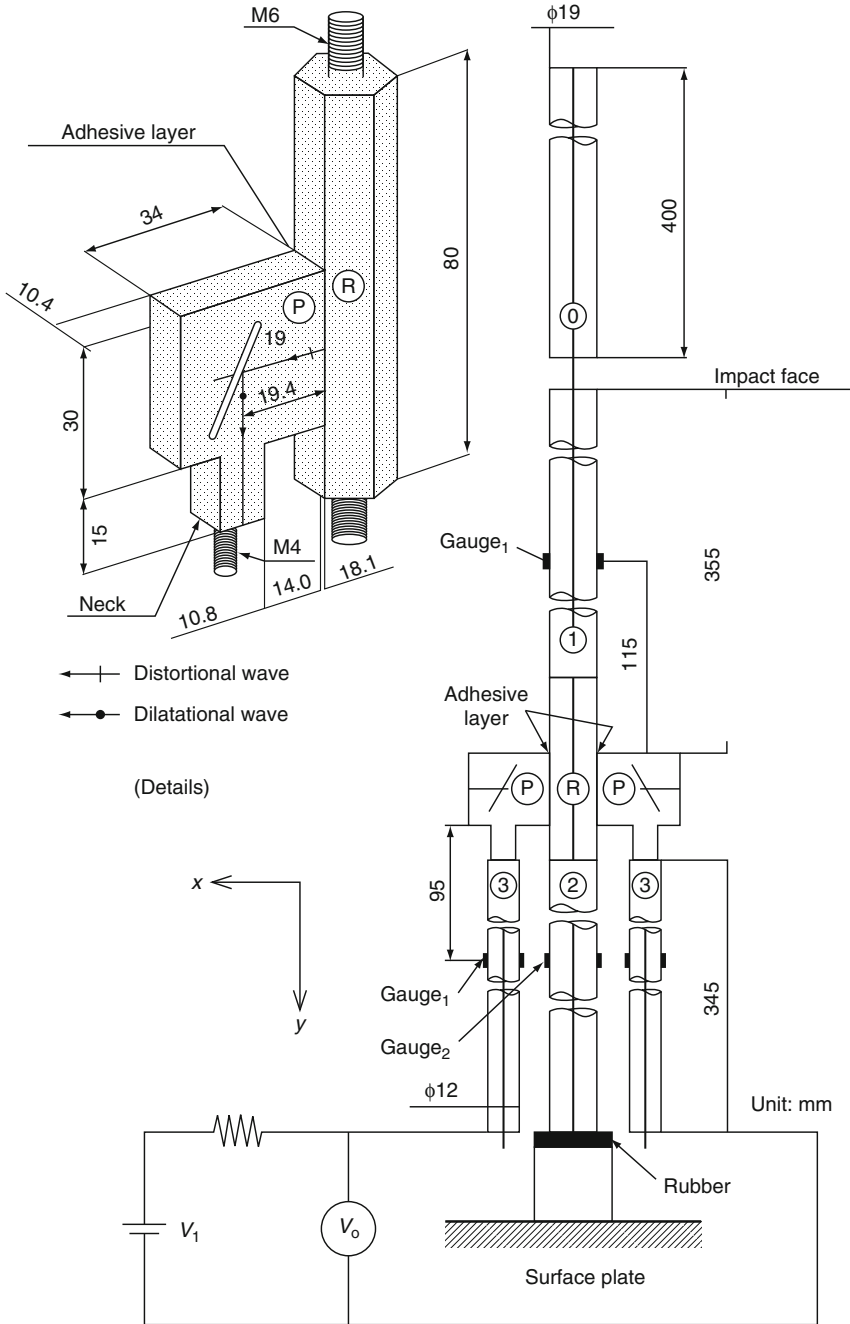
Fig. 14 Test rig to measure the impact strength of adhesive layers (From Kihara et al. 2003, copyright Elsevier)

adhesive stiffness and a 1.83 times lower energy in case of butt joints (respectively, 6.13 and 1.29 times in case of lap-shear joints).

21.5   Other Test Methods

In addition to the test schemes described in the previous sections, some other methods have been applied to test adhesives and joints under impact loading. Most of them are based on schemes that reprise static cases, for the geometry of the specimens or the loading system. The reason for this is not only to recover known cases but – most of all – to evaluate easily the changes in the joint response induced by the loading rate.

21.5.1 Fracture Energy

Regarding the measurement of the adhesive fracture energy G_c, under impact (or, in general, dynamic) conditions, the double cantilever beam test and the tapered double cantilever beam test (Fig. 15) must be adapted to account for the effect induced by the loading rate. Indeed, in statics the base for the measurement is the formula (Williams 1984):

$$G_c = \frac{P_c^2}{2b} \frac{dC}{da} \qquad (5)$$

Fig. 15 Double cantilever beam specimen (**a**) and tapered double cantilever beam specimen (**b**)
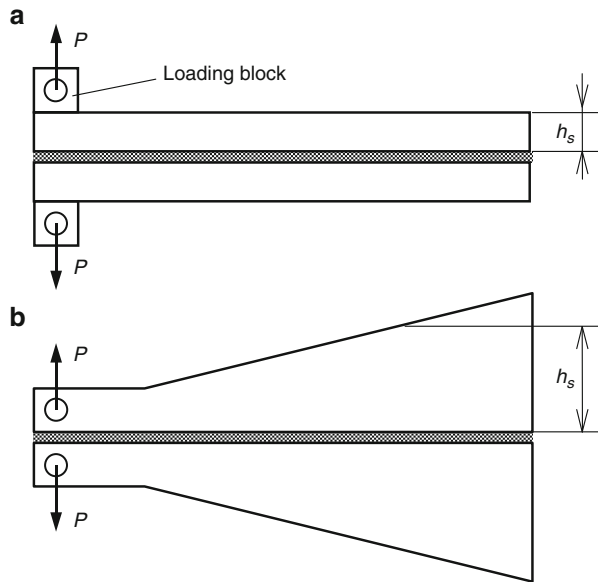
where P_c is the critical load for crack propagation, b is the joint width, a is the crack length, and C is the specimen compliance, i.e., the displacement to force ratio (δ/P). In case of an impact test, the main problem which arises in evaluating the fracture energy is that (as already remarked previously) the force-displacement curve exhibits strong oscillations and, therefore, it is tricky to read from it the relevant information. To avoid this problem, expressions that do not directly make use of load values must be adopted, such as for the double cantilever beam specimen (Kinloch 1997):

$$G_c = \frac{3}{16} \frac{F}{N^2} \frac{\delta_c^2 h_s^3 E_s}{(a + \chi_1 h_s)^4} \tag{6}$$

where F and N are correction factors which, respectively, account for the large deflection of the beam and the stiffening effect of the loading block at the ends of the arms, χ_1 is another correction factor accounting for beam root rotation, and h_s and E_s are, respectively, the height of the beams and Young's modulus of the substrate material. The critical displacement for crack propagation δ_c and the crack length a can be monitored by means of an optical system, as long as the test goes on. In the case of the tapered double cantilever beam specimen, the formula accounts also for the variable beam height.

A sophisticated analysis about the measurement of the fracture energy at high rate of loading has been presented by Blackman et al. (2009). These authors have used the double cantilever test and the tapered double cantilever test to evaluate the behavior of an epoxy adhesive, under loading conditions varying from quasi-static to 15 m/s. The experimental setup includes a hydraulic actuator to apply the load, a high-speed camera, and the suitable electronic devices for measuring, amplifying, processing, and storing the data (Fig. 16). Four different types of crack growth have been identified in this work, namely, (1) slow-rate stable, (2) slow-rate unstable, (3) fast-rate unstable, and (4) fast-rate stable. Here, "stable" is termed the case of steady propagation, while "unstable" is a discontinuous growth, showing sequences of arrest and propagation. It is interesting to notice that the unstable crack growth can occur at intermediate load rate in the tested range; the difference between slow rate and fast rate depends on whether the kinetic energy of the specimen arms is negligible or not with respect to the fracture energy of the adhesive. It is also remarkable that, at the highest load rate adopted in the tests, the crack growth is again stable; obviously in this case the dynamic effects (importance of the kinetic energy, uncertainty on the measured load) are important. For instance, in case of fast-rate loading and double cantilever beam specimen, the formula for the corrected fracture energy (i.e., accounting for the dynamic effects) is

$$G_{Ic} = \frac{3}{4} \frac{Eh^3 (V/2)^2 t^2}{(a + \Delta_I)^4} \frac{F}{N^2} - \frac{33}{140} \frac{Eh(V/2)^2}{c_L^2} \tag{7}$$
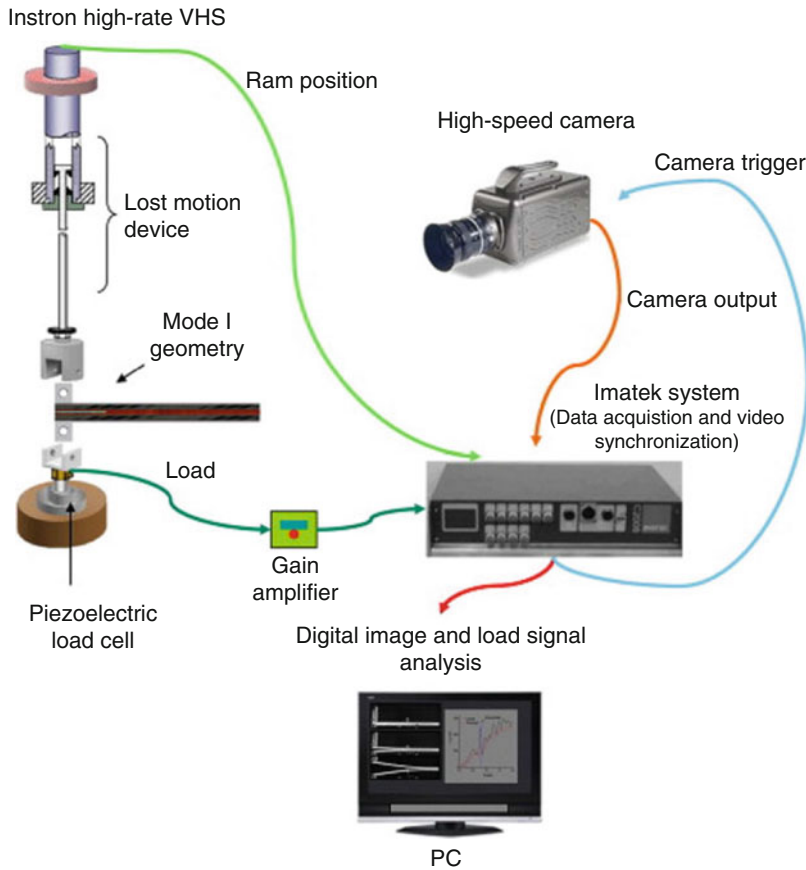
for type 3 crack growth and

Fig. 16 Experimental setup for high rate testing of adhesives under high rate of loading (From Blackman et al. 2009, copyright Elsevier)

$$G_{Ic} = \frac{3}{4} \frac{Eh^3(V/2)^2 t^2}{(a + \Delta_I)^4} \frac{F}{N^2} - \frac{111}{280} \frac{Eh(V/2)^2}{c_L^2} \tag{8}$$

for type 4 crack growth. In both Eqs. 7 and 8, E is Young's modulus of the substrate material, h is the height of the beam, V is the velocity applied by the actuator, t is the time, a is the crack length, Δ_I is the correction factor for beam root rotation, F and N are – again as in Eq. 6 – the correction factors for large deflection of the beam and stiffening effect of the loading blocks, and c_L is the longitudinal wave speed in the substrate material. The first term in Eqs. 7 and 8, which can be obtained from Eq. 6, has the meaning of energy calculated as in static conditions, from which the second term, corresponding to the kinetic energy of the beams, is subtracted. Analogous formulae, of higher complexity due to the non-constancy of the beam section, are available for the tapered double cantilever beam specimen (see again Blackman et al. 2009).

## 21.5.2 Drop-Weight-Based Tests and Alternative Tests

Also in the field of adhesive joining, drop-weight machines are probably the test rigs that have been used first to generate impact conditions.

Beevers and Ellis (1984) have carried out tests on joint specimens fabricated both from mild steel and aluminum coupons, bonded with a toughened epoxy. A drop-weight machine equipped with a strain-gage transducer has been used for impact testing. Compared to the static case, at 4 m/s impact, the steel joints have exhibited a significant increase in ultimate load, while only a small change has been observed for the aluminum joints. This is ascribed to the different strain rate response of the two materials.

Jordan (1988) has described the use of a special drop-weight testing machine, defined "instrumented guillotine." Its peculiar features are the use of a counterweight to adjust the impact energy, from a maximum of 800 J to values lower than 100 J, and a striker of linear shape. The apparatus has been used to test sandwich-type specimens, comparing the impact behavior of epoxy- and acrylic-bonded joints with riveted or spot-welded ones.

Regarding the measurement of the impact strength in terms of force or stress, a first case is represented by the simple butt joint of hollow cylinders, loaded axially in tension. A thorough evaluation of it has been presented by Sawa et al. (2002, 2003). In these works, impact tests have been carried out on specimens made of two hollow steel cylinders bonded together (Sawa et al. 2002) and a hollow steel cylinder bonded to a hollow aluminum cylinder (Sawa et al. 2003); in both works the adhesive is an epoxy, and the outside and inside diameters of the cylinders are 15 and 5 mm, respectively. Figure 17 shows the experimental setup; it can be noticed

Fig. 17 Schematics of the impact test on cylindrical butt joints used by Sawa et al. (2002) and Sawa et al. (2003)
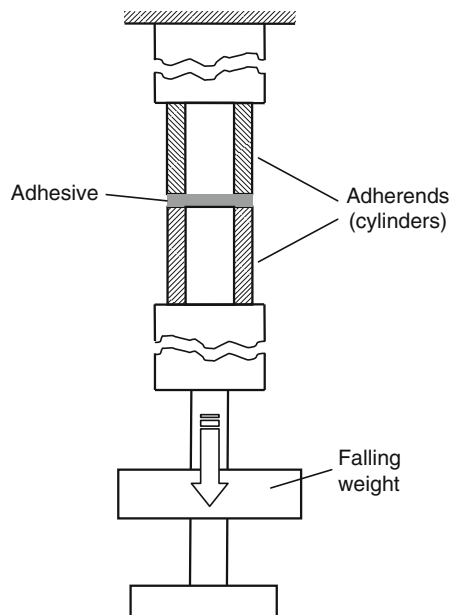
that the load is applied by releasing, from a chosen height, a weight that hits the flange of the coaxial guide bar which, in turn, applies the tension to the lower cylinder. The measurements are taken by means of strain gages placed on the surface of the cylinders, close to the bond. The papers describe in detail the finite element elastoplastic modeling of the experiments, which aims at assessing the state of stress and strain in the adhesive; in particular, the peak stress occurs at the outside edge of the interface, its value decreases as the adhesive thickness increases (while the opposite trend occurs under static loading). When the specimens are formed by two steel cylinders, fracture always occurs at the lower adhesive/metal interface, which is reached first by the pulse arriving from bottom; in case of dissimilar adherends, fracture occurs at the adhesive/aluminum interface. The impact energy is higher in case of steel-aluminum specimens than in case of steel-steel, about 1.7 times if the lower cylinder is of aluminum, and about 1.5 times if the upper cylinder is of aluminum. Conversely, the opposite behavior is observed for the peak load, which is higher in case of steel-steel specimen.

Another notable case is the study of lap joints under different impact conditions. A reason in favor for this choice is that the single-lap joint is the commonest type of specimen used for static testing; thus it appears straightforward to test the same geometry under dynamic conditions, to evaluate the influence of the loading rate without introducing additional (and possibly misleading) effects due to a change of geometry.

Goglio and Rossetto (2008) have tested single-lap specimens using a modified instrumented Charpy pendulum (Fig. 18). The specimen is mounted on the hammer by means of a fixture that pulls its front half; the back half of the specimen is connected to a transverse tail. When, at the end of the fall, the hammer reaches its lowest position, the tail impacts a pair of stoppers fixed to the pendulum base, and
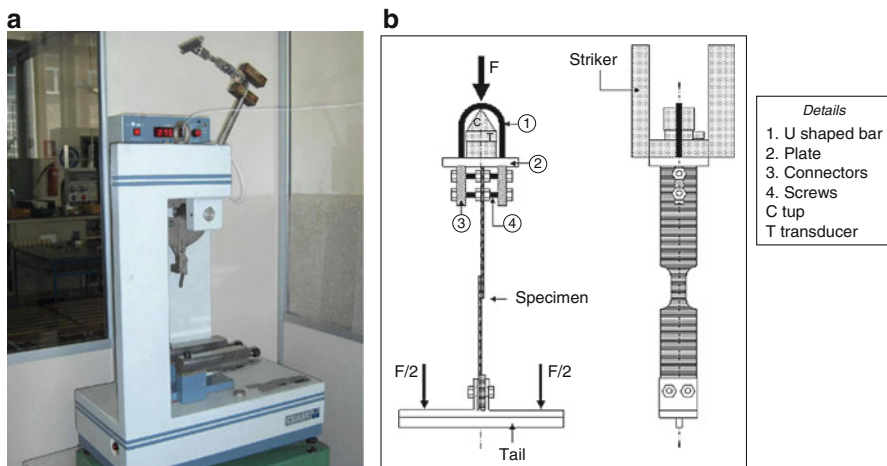

Fig. 18 Charpy pendulum adapted to test lap joints: (**a**) overall view; (**b**) fixation of the specimen on the hammer (From Goglio and Rossetto 2008, copyright Elsevier)

this causes tension in the specimen. This scheme is opposite to that used in other works, such as by Harris and Adams (1985), in which the specimen is fixed at its back half to the pendulum base; the hammer during its fall hooks the front half specimen, thus applying the traction. The hammer is instrumented with a piezoelectric load cell, so that the force can be measured and recorded. The scheme reproduces, in dynamic conditions, the usual stress state of the single-lap joints, with shear and peel stresses concentrated at the overlap ends. It is worth noting that in this kind of test, although the hammer speed is moderate (some m/s), for adhesive layers of some tenths of mm the magnitude of the resulting shearing strain rate is 10^3 s^{-1}.

In the work by Goglio and Rossetto (2008), several combinations of bonded length (3, 8, 12.5 mm), adherend thickness (1.5, 3 mm), and adhesive thickness (0.5, 1 mm) have been tested, with the aim of producing failure under different blends of stress. In all cases the adherends were of mild steel, and the adhesive was a bicomponent epoxy; failure occurs in the adhesive, while the adherends remain undamaged. The main result is represented by the graph of Fig. 19 in which (with the same style as of Fig. 13) the maximum values of stress (calculated with a mono-dimensional model) corresponding to failure conditions are reported. Also the points corresponding to failure under static loading are plotted for comparison. The increase of stress values changing from static to impact conditions is evident; regarding the effect of the adhesive thickness, it must be remarked that the thinner layer, under the same speed applied by the pendulum, undergoes a higher strain rate.

A drawback of the use of a pendulum is that, due to the transfer of energy from the hammer to the specimen, the speed during the impact is not exactly constant (although the speed drop is usually limited). A solution to avoid this, used by Cayssials and Lataillade (1996), is to replace the pendulum with a heavy rotating
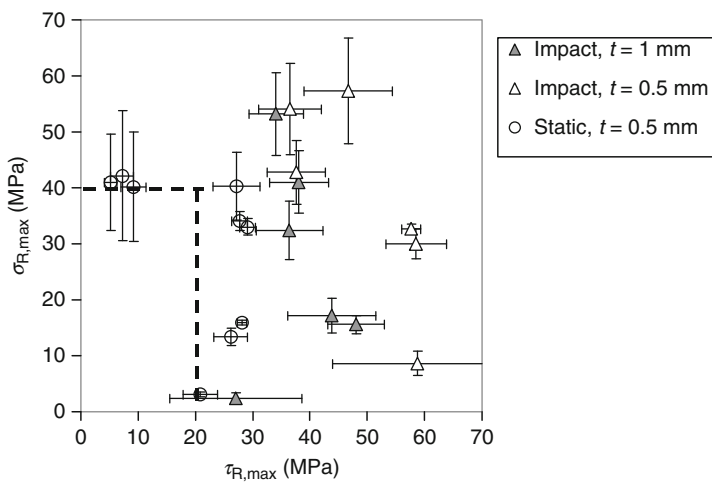

Fig. 19 Failure locus described by normal and tangential maximum stresses; bars show ± 1 standard deviation (From Goglio and Rossetto 2008, copyright Elsevier)
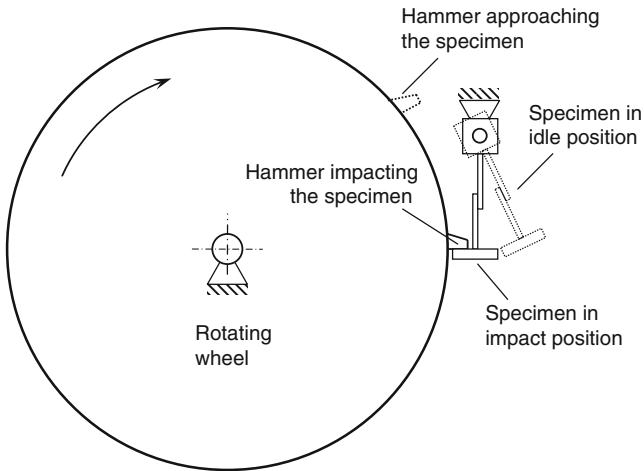
Fig. 20 Schematic of the inertia wheel used by Cayssials and Lataillade (1996)

wheel, termed "inertia wheel," schematized in Fig. 20. Once the wheel (driven by a motor) has reached the desired speed, the specimen is set in position and struck by a hammer fixed at the wheel periphery. Due to the high moment of inertia of the wheel, the reduction of speed is negligible. Also Marzi et al. (2015) have used a rotary device, to assess the dynamic strength of bonded T-peel specimens. Their work has especially aimed at evaluating the performance of a 3D optical systems designed to measure the deformations.

A further alternative to the drop-weight scheme is the use of the "quick crusher," mounted on a standard tensile testing machine. With this device, the jaws are initially kept open, while the crosshead accelerates; then, they suddenly clamp the specimen, applying an impact load. Schiel et al. (2015) adopted it to assess the impact behavior of bonded joints between zinc-coated or painted sheet metal, typical of the automotive industry. They have found that, in joints fabricated with epoxy adhesives, the weak point is the metal-coating interface or the coating itself.

Another mode in which a lap joint can be impact loaded is out of plane bending. The reason of interest for this case is that, although bonded panels are designed and tested considering their service condition (which, usually, causes in plane loading), the capability of sustaining unexpected transverse impact loads must be assessed as well. For instance, in aerospace construction cases of interest are impacts with debris (in service) and fall of tools (during manufacturing or maintenance).

To validate a spring-mass model of a lap joint under three-point bending, Pang et al. (1995) have carried out low-velocity impact tests on joints of composite laminates, hit by the hemispherical impactor of a drop tower instrumented with semiconductor strain gages to measure the force. Two different overlap lengths and two different adherend thicknesses have been used in the experiments; also the drop height has been varied to obtain different velocities in the range 3.6–4.6 m/s approximately. In this way, the authors have measured the force time history in the

Fig. 21 Schematic of the transverse impact tests carried out by Higuchi et al. (2002)
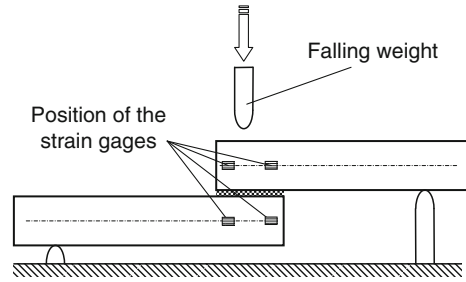
impacts and, in particular, the peak force, to correlate it with joint geometry and impact velocity.

Similar experiments have been carried out by Higuchi et al. (2002) to validate the finite element analysis of a single-lap joint. The specimens used in this work were mild steel plates bonded with an epoxy adhesive; strain gages have been applied (in longitudinal direction) on the mid thickness of the adherends to measure the local strain during the impact (see Fig. 21); the impact velocity was about 1 m/s. The goal of this work is to assess the stress distribution on the adherend-adhesive interface which is obtained from finite element results, since it is not possible to measure it directly (the model is validated by comparing its results in points at mid thickness of the adherends, where experimental measurements have been obtained with strain gages). The main findings concern the maximum principal stress σ_1, which attains its maximum near the edge of the interface of the adhesive with the upper (impacted) adherend. It has been noticed that, unlike the case of static loading, such principal stress increases for increasing adherend Young's modulus, overlap length, and adherend thickness; this is due to the fact that, increasing these parameters, the joint reacts with higher stiffness to the displacement imposed by the impactor. Conversely, increasing the adhesive thickness, the principal stress decreases, as it happens in the case of static loading.

Vaydia et al. (2006) have considered the case of bonded composite panels, again impact loaded in three-point bending. In this work, the specimens were epoxy-carbon strips manufactured from carbon fabric; three distinct types of adhesives were used, namely, two different bicomponent epoxies and a nanoclay-reinforced (7%) epoxy. The latter case is considered to test the strength of an adhesive composition suitable to improve its performance under harsh condition (moisture uptake), although such high nanoclay content is expected to reduce the mechanical properties. Impact is applied by the tip of a drop-weight machine, with the setup shown in Fig. 22; the velocity is in the range 1–2 m/s. An extensive finite element analysis was carried out to understand the response of the joint to this loading condition. Model results confirm that there is a strong stress concentration at the ends of the overlap; in particular the peel component has a negative peak at the end of the upper (i.e., impacted) adherend and a positive peak at the end of the unloaded adherend. This fact can be understood by means of a simple argument about the rigid body relative rotation of the two adherends induced by the impact. Also, the shear stress peaks at the ends of the overlap, but the intensity is lower. The examination of
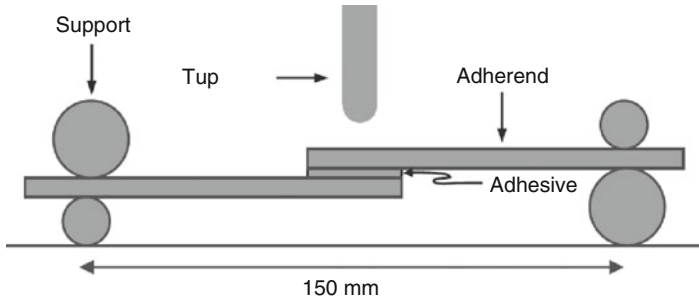
Fig. 22 Schematic of the transverse impact testing of bonded composites (From Vaidya et al. 2006, copyright Elsevier)

the broken specimen suggests that the crack is initiated by the shear stress and then propagated by the dominant peel stress.

In addition to the strength of adhesives under impact, also the properties related to dynamic deformability are of interest. Sato and Ikegami (2000) have studied the cases of lap joints and scarf joints subjected to axial impact loads. Preliminarily, they have measured the attenuation of the axial strain waves in a special specimen of epoxy adhesive, manufactured (by molding the adhesive resin) as a cylinder of length 900 mm and diameter 20 mm. From these results, the complex compliance of the material was obtained and, in turn, used to identify the parameters of a five-element Voigt model of viscoelasticity. These material data have been introduced in the finite element simulation of the impact tests on the joints. The joints used in these tests were made by aluminum strips 4 mm thick – bonded with the abovementioned epoxy – and adopting three different kinds of geometry, namely, single lap (square ended), tapered, and scarf. The equipment used for carrying out the tests is shown in Fig. 23; the impact bar driven by the cam hits the upper end of the specimen applying the impact load. The main difference between the types of specimen is that in the lap joint, the offset of the adherend midplanes creates a bending moment, from which high stresses originate; in the tapered lap joint this effect is mitigated; for the scarf joint the adherends are aligned and the stresses propagate easily through the joint. The measurements confirm these remarks; in the tapered lap joints (overlap length 100 mm, taper length 50 mm), the peak stresses are reduced about 50% with respect to the single lap (overlap length 100 mm); in the case of scarf joint, the stresses are even much smaller and smoothly distributed, since the stress concentration is relieved.

A comparison of the effect of the strain rate on the mechanical response of a brittle and a ductile adhesive has been carried out by Sugaya et al. (2011), using a drop-weight machine in the tests at higher rates. These authors have found that for the brittle adhesive, the elastic modulus is insensitive to the strain rate, while under increasing strain rate, the tensile strength and the strain at failure increase (the latter remained anyhow small, as only the elastic range was extended). The effect of the strain rate on the ductile adhesive is to increase the tensile strength and to reduce the strain at failure.
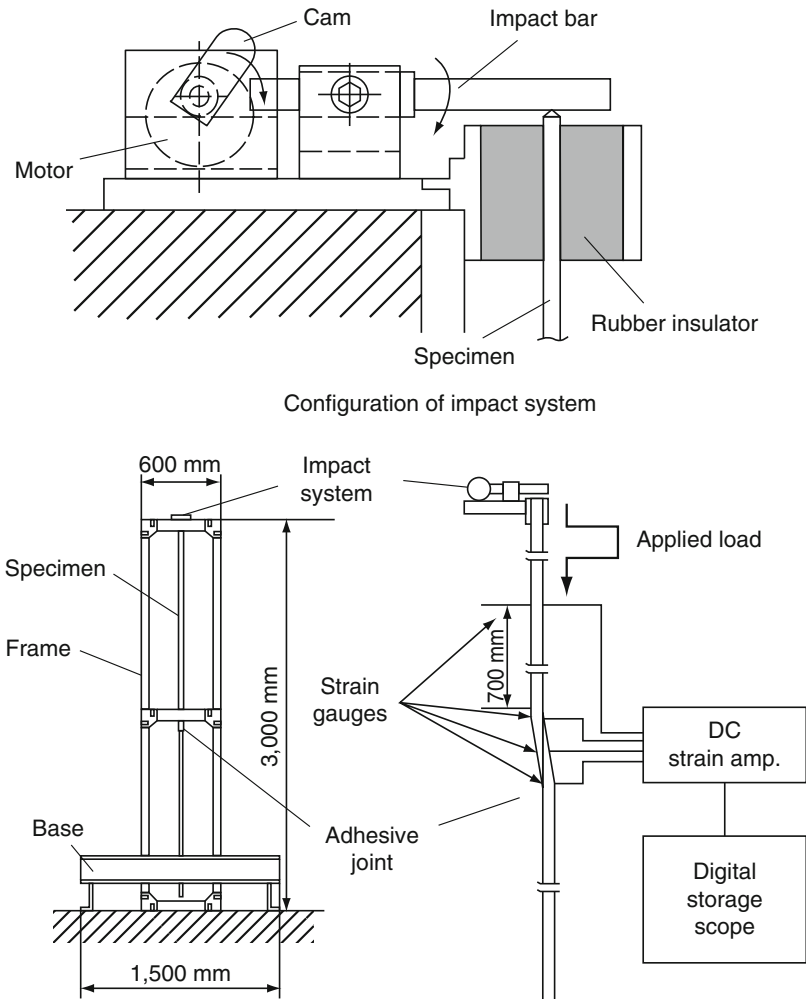
Fig. 23 Experimental equipment for impact testing of lap and scarf joints (From Sato and Ikegami 2000, copyright Elsevier)

Liao and Sawa (2011) have studied the strength of steel shafts bonded in epoxy hollow cylinders and subjected to axial push-off loads. To support their finite element modeling, they have carried out experiments on a drop-weight machine, and the strains in the cylinder have been measured with strain gages. Good agreement has been found between calculated and measured results.

Al-Zubaidy et al. (2012) have tested experimentally the impact behavior of adhesive bonds between steel plates and CFRP sheets, mainly used for retrofitting existing steel structures. Double strap specimens with different numbers of CFRP layers, fabricated with an epoxy adhesive, have been subjected to impact loads up to

5 m/s applied by means of a drop-weight machine. The results have shown the existence of an effective bond length, above which a further increase in overlap does not increase the ultimate load. Compared to the static strength, the impact strength has increased at loading rate 3.5 m/s and decreased at higher rates.

Liao et al. (2013) have modeled single-lap adhesive joints with dissimilar adherends (aluminum-steel) subject to tensile impact and carried out experiments on a drop-weight machine. In the finite element calculations, the Cowper-Symonds model has been used to account for the strain rate dependence. Finite element and experimental results have agreed in showing that (unlike the case of static loading) under impact the failure starts at the interface of the stiffer adherend.

By investigating the behavior of a phenolic resin adhesive blended with rubber, using a pendulum-like testing machine, Adachi et al. (2015) have found an experimental validation of the principle of equivalence between strain rate and temperature. They advance that impact strength could be predicted by applying the principle.

Kadioglu and Adams (2015) have studied the behavior of a flexible viscoelastic tape for automotive application. Single-lap joints of high-strength steel have been tested on a pendulum equipped with a load cell and a laser for measuring the displacement. Compared to static response, an increase of more than twice in adhesive shear strength has been noticed at 1.4 m/s impact speed.

The impact behavior of a pressure-sensitive adhesive has been studied by Hayashida et al. (2015) using butt joint and double cantilever beam specimens and measuring the deformations by means of a high-speed camera. Transparent adherends have been used to observe cavitation and fibrillation, which are the phenomena controlling ductility for this adhesive. It has been noticed that under increasing strain rate, the strength of the butt joints increases, while the fracture energy of the double cantilever beam specimens decreases. This is ascribed to the fact that at high strain rate, the pressure-sensitive adhesive becomes brittle due to viscoelastic effects.

Silva et al. (2016) have studied joints for automotive use, fabricated by combining adhesives of different types, ductile or brittle, as sketched in Fig. 24. The ductile and soft adhesive is placed in the ends of the joint overlap, to smoothen the stress concentrations, while the brittle and hard adhesive is set in the middle of the joint. Impact tests carried out with a drop-weight machine have shown that such a design exploits the best of the two kinds of adhesives, in terms of ultimate load (as shown in Fig. 25) and energy.

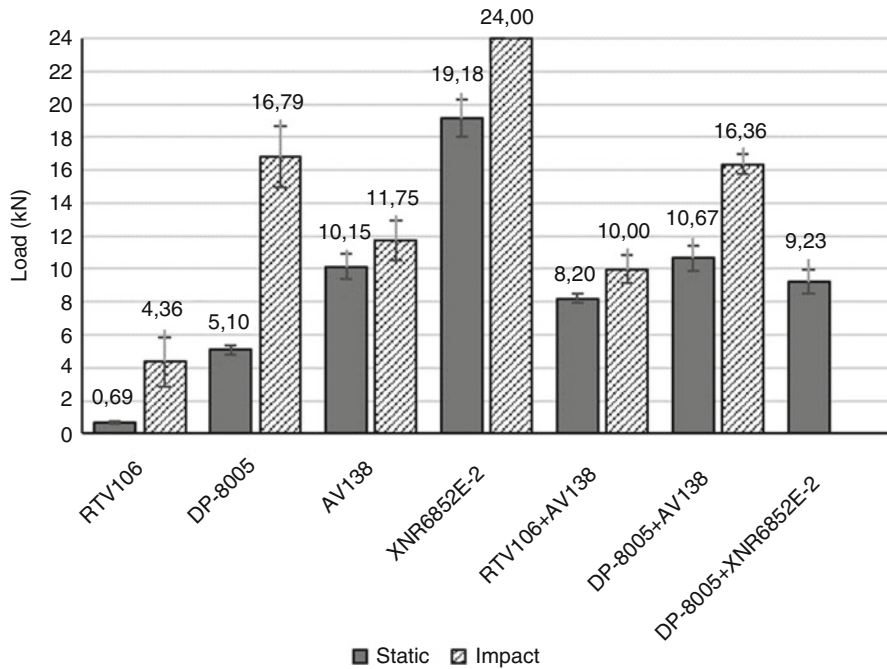Fig. 24 Schematic of mixed adhesive joint
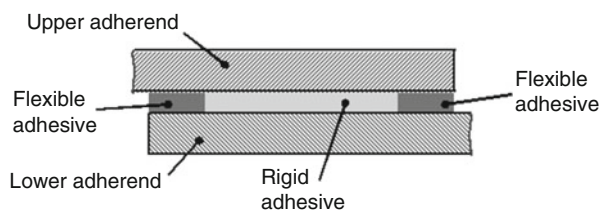
Fig. 25 Average maximum load comparison between static and impact conditions (From Silva et al. 2016, copyright Latin American Journal of Solids and Structures)

21.6 Conductive Adhesives

A field of application that has received attention in the last two decades is the use of conductive adhesives to replace soldering in electronic applications. Such change can bring advantages mainly of ecological type, eliminating the dangerous substances that can be produced by the soldering process and the need for energy to melt the solder. An important advantage given by adhesive joining is that the pitch between neighboring contacts can be shorter compared to the case of soldering, and this is beneficial as far as miniaturization is concerned. Apart from the technological differences introduced by adopting a new technology, the main concerns related to the use of adhesives in this field are unstable contact resistance and impact strength.

Zwolinsky et al. (1996) have reported results obtained by a project of the National Center for Manufacturing Sciences (NCMS), carried out in the early 1990s to assess the suitability of 25 conductive adhesives available on the market at that time. In particular, regarding the assessment of the impact strength, experiments of two types were performed. In the first phase of the project, specimens made with a plastic leaded chip carrier (PLCC) bonded on a coupon were dropped repeatedly from two

different heights, respectively, 0.457 m (18 in.) and 0.914 m (36 in.), recording the number of drops needed to detach the PLCC for each height. In the second phase, drop tests were carried out in specimens formed by a board containing a collection of components, joined by bonding. Each specimen was subjected to three drops from the height of 0.914 m (36 in.). The presence of damage due to the impacts is noticed both by visual inspection and by measurement of the electrical resistance. The result of this series of tests was that the commercial adhesives used at that time were not capable to withstand the impact condition. The authors recommend evaluating the impact performance of an adhesive with a series of 6 drops from 1.52 m (60 in.), with a specimen formed by a bonded PLCC. This recommendation is one of the bases of the NCMS specification for solder replacement adhesives.

Another study of the impact performance of the conductive adhesives was carried out by Daoquiang and Wong (1999). To overcome the poor impact performance of the commercial conductive adhesives, these authors have proposed an adhesive of new formulation containing epoxy-modified polyurethane resin and bisphenol-F. The adopted impact test method is again the one proposed by NCMS and mentioned above (Fig. 26); the channel in which the specimen under test is dropped has the aim of avoiding rotation, thus forcing the part to impact the ground with a defined edge. In their work, these authors have also measured the internal damping of the adhesive, and they have noticed that the materials having high loss factor (tan δ) are also the most capable to withstand the impacts.

It is evident that the abovementioned experiments obtain, as outcome, the simple result of failure or survival of the specimens. No insight is found about the stress state in the bonds; furthermore, the drop test assesses the strength of the bonded

Fig. 26 Schematics of the NCMS drop test for bonded electronic components
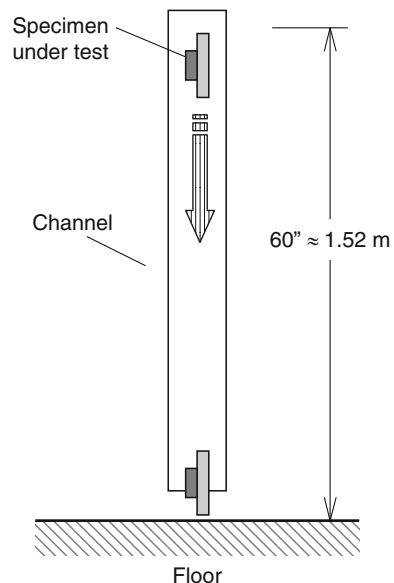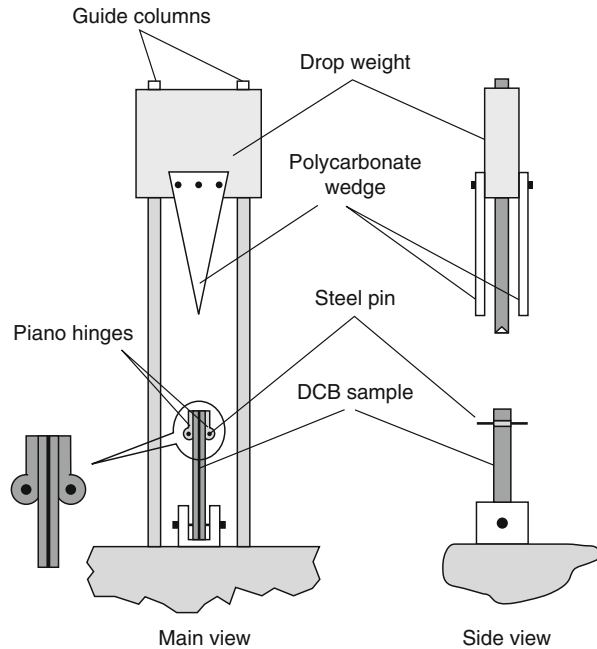
Fig. 27 Falling wedge test arrangement for conductive adhesives (From Xu and Dillard 2003, copyright IEEE)

specimen, not of the adhesive itself. More recent works aim at studying the impact behavior of the bonded electronic parts with the methods of fracture mechanics or structural dynamics.

Wu et al. (2003) have tested surface mount joints in printed circuit boards, comparing the behavior of an isotropic conductive adhesive with a traditional lead-tin soldering alloy. Joint specimens have first undergone impact on a modified Hopkinson bar, specialized to create three-point bending conditions. Then, after the impact, the specimens (if not already failed) have been destructively tested under shear to assess their residual strength. It has been noticed that the residual shear strength of the joints decreases under increasing strain rate. Compared to the soldering alloy, the adhesive has exhibited lower strength, which nonetheless can be considered satisfactory for practical applications.

Xu and Dillard (2003) have studied the impact strength of conductive adhesives by means of a new impact test, termed falling wedge test (Fig. 27). Its principle is similar to that of the double cantilever beam: a pair (because of the symmetry of the specimen) of wedges fall along a drop tower and with its motion splits apart the two substrates of the bonded joint, mounted vertically on the base of the test rig. To avoid the typical problems related to impact load measurement (already recalled in this section), no load measurement is carried out directly. In the test rig the deformation of the sample is captured by means of a high-speed camera, so that the displacement of the end points and the deformed shape of each beam are obtained from the images. The fracture energy is calculated as

$$G_c = \frac{9\delta_0^2 EI}{4Ba^4} \tag{9}$$

where δ_0 is the opening displacement, E is Young's modulus of the substrate, I is the moment of inertia of the beam section, B is the beam width, and a is the crack length. It is easy to notice that Eq. 9 is a simplified version of Eq. 6, in which the correction factors are neglected. The specimens are coupons of printed circuit boards bonded in their central part (by means of a spacer); the adhesives are three different silver-filled epoxy adhesives, especially produced for this research. The tests have been carried out at several temperatures, between $-70\ ^\circ$C and $90\ ^\circ$C, at a fixed impact speed of about 1.6 m/s. It has been observed that the results are influenced by the temperature when the glass transition temperature (T_g) of the adhesive is in the considered range; in particular a maximum of G_c has been noticed for a test temperature close to the T_g of the adhesive under consideration. These series of tests have confirmed the correlation between the loss factor of the material and the fracture energy.

Rao et al. (2004), reprising the case considered in a work mentioned above (Daoquiang and Wong 1999), have added the study of the first natural frequencies and mode shapes of an electronic packaging formed by a PLCC bonded to a coupon of printed board. From the theoretical viewpoint, an ideal impulse would excite all natural frequencies of the system. This study has considered the first ten natural frequencies, whose range of values, obtained with a finite element model, is extended up to 2 kHz approximately. The impact behavior of the adhesive is adequate if its damping is high enough to dissipate energy over the whole range. The authors have measured the loss factor of four different adhesives, in a frequency range from 0.1 to 3,000 Hz. Comparing these measurements with the results obtained from the drop tests, it has been once again observed that the capability of withstanding the impact is related to the internal damping.

A comprehensive state-of-the-art review on conductive adhesives has been presented by Irfan Mir and Kumar (2008), which considers the main related problems and, among these, the aspects regarding impact strength.

21.7   Response to Environmental Conditions

A quite peculiar case is that considered by Park and Kim (2010), who have tested single-lap joints between composite panels subjected to transverse impact of ice spheres, to reproduce the effect of hailstones against an aircraft or other structures exposed to the phenomenon. The experiments and the related finite element simulations have shown that damage occurs if the kinetic energy of the impactor exceeds a threshold. The most important failure mode is delamination, both for panels and joints; however, also adhesive failure can occur. Examination of the specimens has shown that the damage is mainly due to the stress concentration related to the joint. Thus, a joined assembly is more susceptible to this type of damage than a monolithic panel.

Zhang et al. (2015) have studied the response to the strain rate after hygrothermal exposure in an experimental study on joints made of metal adherends (steel, aluminum) bonded with a toughened epoxy. By comparing the response at several crosshead speeds with the quasi-static conditions, they have noticed that: loading rate and aging can be regarded as independent influencing factors (with negligible interaction); the ultimate load is increased by loading rate and decreased by the hygrothermal exposure. The effects of these two factors can be accounted for by means of a linear empirical formula, to predict the resulting strength.

21.8   Conclusions

This chapter has described the main tests used to assess the impact strength of adhesives and joints, considering both those foreseen by international standards and those appeared in research papers. The main types of test rigs used in the experiments are pendulum, falling weight and Hopkinson bar, or evolutions of these.

The major conclusions of this survey are the following:

1. Of the two standard test methods, the block impact (ASTM D950) is the easiest to carry out and does not require sophisticated equipment, but the only result it gives is the absorbed energy. Moreover, the specimen made of bonded blocks is far from the case of a typical joint, made of thin substrates; thus, this test can give (at best) only a comparison between different adhesive systems. The study by Adams and Harris (1996) has shown that even small errors of alignment can deeply modify the stress profile in the specimen; thus also the use of this test for comparison between adhesives is questionable.

2. The other test foreseen by a standard is the wedge peel impact (ISO EN 11343). Although in this case the arrangement is more representative of a real joint, the immediate answer given by the test rig is a property (energy) of the system formed by specimen and adhesive. Sophisticated data processing is required to extract further information and correlate the result of this test with the adhesive fracture energy G_c, as done by Blackman et al. (2000). These authors have also shown that in case of unstable crack growth, the ISO standard procedure to process the force time history can produce wrong results. They have also found that the effect of the friction between wedge and strips plays a minor role, compared to G_c.

3. When the mechanical properties of the adhesive at high loading rate (strain rate $10^3 \, \text{s}^{-1}$) are sought, the appropriate test rig is the Hopkinson bar. This apparatus is suitable to test specimens of adhesive under compression in straightforward manner; tests under tension can be carried out with modifications of the basic scheme. Also simple joints can be tested, by properly adapting the ends of the bars. In the last decade, this equipment has become more and more popular and adapted to tests specimens of various shapes (e.g., lap, pin-collar) under different loading conditions (e.g., tension, bending, shear).

4. In the research works presented in the literature, many test rigs are based on the falling weight scheme; alternatively, the impact is applied by a hydraulic ram. In most cases, the specimens are single-lap joints, impacted axially (i.e., in tension) or transversally (i.e., in bending). Usually, in this kind of tests, the impact force is measured by a load cell embedded in the impactor, and the time history is recorded electronically. The typical problem of this measurement is that what is actually measured depends also on the dynamic response of the system formed by specimen and test rig; thus the observed oscillation is not only due to the start and growth of the crack in the joint. For this reason, when the determination of fracture mechanics properties (usually G_c) is sought, the use of force measurements is avoided, and the displacement is preferred instead.

As a final remark, it can be added that frequently the experimental studies on the behavior of adhesive or joints under impact are presented together with finite element simulations. This interaction between testing and modeling is, in this field, especially needed, since the possibility of direct measurement of the desired quantities is limited and hindered by the complications introduced by the dynamic response of the tested system.

References

Adachi T, Kataoka T, Higuchi M (2015) Predicting impact shear strength of phenolic resin adhesive blended with nitrile rubber. Int J Adhes Adhes 56:53–60

Adams RD, Harris JA (1996) A critical assessment of the block impact test for measuring the impact strength of adhesive bonds. Int J Adhes Adhes 16:61–71

Adamvalli M, Parameswaran V (2008) Dynamic strength of adhesive single lap joints at high temperature. Int J Adhes Adhes 28:321–327

Al-Zubaidy H, Al-Mahaidi R, Zhao X-L (2012) Experimental investigation of bond characteristics between CFRP fabrics and steel plate joints under impact tensile loads. Compos Struct 94:510–518

ASTM D950-03, Standard Test Method for Impact Strength of Adhesive Bonds. ASTM Int

Beevers A, Ellis MD (1984) Impact behaviour of bonded mild steel lap joints. Int J Adhes Adhes 4:13–16

Bezemer AA, Guyt CB, Vlot A (1998) New impact specimen for adhesives: optimization of high-speed-loaded adhesive joints. Int J Adhes Adhes 18:255–260

Blackman BRK, Kinloch AJ, Taylor AC, Wang Y (2000) The impact wedge-peel performance of structural adhesives. J Mater Sci 35:1867–1884

Blackman BRK, Kinloch AJ, Rodriguez Sanchez FS, Teo WS, Williams JG (2009) The fracture mechanics of adhesives under high rates of loading. Eng Fract Mech 79:2868–2889

Bragov AM, Lomunov AK (1995) Methodological aspects of studying dynamic material properties using the Kolsky method. Int J Impact Eng 16:321–330

Cayssials F, Lataillade JL (1996) Effect of the secondary transition on the behaviour of epoxy adhesive joints at high rates of loading. J Adhesion 58:281–298

Challita G, Othman R (2010) Finite-element analysis of SHPB tests on double-lap adhesive joints. Int J Adhes Adhes 30:236–244

Challita G, Othman R, Casari P, Khalil K (2011) Experimental investigation of the shear dynamic behavior of double-lap adhesively bonded joints on a wide range of strain rates. Int J Adhes Adhes 31:146–153

Chen W, Lu F, Cheng M (2002) Tension and compression tests of two polymers under quasi-static and dynamic loading. Polym Test 21:113–121

Daoqiang L, Wong CP (1999) High performance conductive adhesives. IEEE Trans Electron Packag Manuf 22:324–330

Forrestal MJ, Wright TW, Chen W (2007) The effect of radial inertia on brittle samples during the split Hopkinson pressure bar test. Int J Impact Eng 34:405–411

Gilat A, Goldberg RK, Roberts GD (2007) Strain rate sensitivity of epoxy resin in tensile and shear loading. J Aerosp Eng 20:75–89

Goglio L, Rossetto M (2008) Impact rupture of structural adhesive joints under different stress combinations. Int J Impact Eng 35:635–643

Goglio L, Peroni L, Peroni M, Rossetto M (2008) High strain-rate compression and tension behaviour of an epoxy bi-component adhesive. Int J Adhes Adhes 28:329–339

Harris JA, Adams RD (1985) An assessment of the impact performance of bonded joints for use in high energy absorbing structures. Proc Inst Mech Eng 199:121–131

Hayashida S, Sugaya T, Kuramoto S, Sato C, Mihara A, Onuma T (2015) Impact strength of joints bonded with high-strength pressure-sensitive adhesive. Int J Adhes Adhes 56:61–72

Higuchi I, Sawa T, Suga H (2002) Three-dimensional finite element analysis of single-lap adhesive joints subjected to impact bending moments. J Adhesion Sci Technol 16:1327–1342

ISO EN 11343 (2003) Adhesives – Determination of dynamic resistance to cleavage of high-strength adhesive bonds under impact conditions – Wedge impact method

Jordan M (1988) The instrumented guillotine impact testing apparatus. Int J Adhes Adhes 8:39–46

Kadioglu F, Adams RD (2015) Flexible adhesives for automotive application under impact loading. Int J Adhes Adhes 56:73–78

Kihara K, Isono H, Yamabe H, Sugibayashi T (2003) A study and evaluation of the shear strength of adhesive layers subjected to impact loads. Int J Adhes Adhes 23:253–259

Kinloch AJ (1997) Adhesives in engineering. Proc Inst Mech Eng Part G 211:307–335

Kolsky H (1963) Stress waves in solids. Dover Publications, New York

Liao L, Sawa T (2011) Finite element stress analysis and strength evaluation of epoxy-steel cylinders subjected to impact push-off loads. Int J Adhes Adhes 31:322–330

Liao L, Sawa T, Huang C (2013) Experimental and FEM studies on mechanical properties of single-lap adhesive joint with dissimilar adherends subjected to impact tensile loadings. Int J Adhes Adhes 44:91–98

Machado JJM, Marques EAS, Campilho RDSG, da Silva LFM (2017) Adhesives and adhesive joints under impact loadings: an overview. J Adhesion. https://doi.org/10.1080/00218464.2017.1282349

Martínez MA, Chocron IS, Rodriguez J, Sànchez Gàlvez V, Sastre LA (1998) Confined compression of elastic adhesives at high rates of strain. Int J Adhes Adhes 18:375–383

Marzi S, Biel A, Hesebeck O (2015) 3D optical displacement measurements on dynamically loaded adhesively bonded T-peel specimens. Int J Adhes Adhes 56:41–45

May M, Hesebeck O, Marzi S, Böhme W, Lienhard J, Kilchert S, Brede M, Hiermaier S (2015) Rate dependent behavior of crash-optimized adhesives – Experimental characterization, model development, and simulation. Eng Fract Mech 133:112–137

Mir I, Kumar D (2008) Recent advances in isotropic conductive adhesives for electronics packaging applications. Int J Adhes Adhes 28:362–371

Neumayer J, Kuhn P, Koerber H, Hinterhölzl R (2016) Experimental determination of the tensile and shear behaviour of adhesives under impact loading. J Adhes 92:503–516

Pang SS, Yang C, Zhao Y (1995) Impact response of single-lap composite joints. Compos Eng 5:1011–1027

Park H, Kim H (2010) Damage resistance of single lap adhesive composite joints by transverse ice impact. Int J Impact Eng 37:177–184

Rao Y, Lu D, Wong CP (2004) A study of impact performance of conductive adhesives. Int J Adhes Adhes 24:449–453

Ravi Sankar H, Adamvalli M, Kulkarni PP, Parameswaran V (2015) Dynamic strength of single lap joints with similar and dissimilar adherends. Int J Adhes Adhes 56:46–52

Sato C, Goglio L (2015) Guest editorial. Int J Adhes Adhes 56:1–2

Sato C, Ikegami K (1999) Strength of adhesively-bonded butt joints of tubes subjected to combined high-rate loads. J Adhes 70:57–73

Sato C, Ikegami K (2000) Dynamic deformation of lap joints and scarf joints under impact loads. Int J Adhes Adhes 20:17–25

Sawa T, Suzuki Y, Kido S (2002) FEM stress analysis and strength of adhesive butt joints of similar hollow cylinders under static and impact tensile loadings. J Adhes Sci Technol 16:1449–1468

Sawa T, Suzuki Y, Kido S (2003) Stress analysis and strength estimation of butt adhesive joints of dissimilar hollow cylinders under impact tensile loadings. J Adhes Sci Technol 17:943–965

Schiel M, Kreling S, Unger C, Fischer F, Dilger K (2015) Behavior of adhesively bonded coated steel for automotive applications under impact loads. Int J Adhes Adhes 56:32–40

Sen O, Tekalur SA, Jilek C (2011) The determination of dynamic strength of single lap joints using the split Hopkinson pressure bar. Int J Adhes Adhes 31:541–549

Silva MRG, Marques EAS, da Silva LFM (2016) Behaviour under impact of mixed adhesive joints for the automotive industry. Lat Am J Sol Struct 13:835–853

Sugaya T, Obuchi T, Sato C (2011) Influences of loading rates on stress-strain relations of cured bulks of brittle and ductile adhesives. J Sol Mech Mater Eng 5:921–928

Tyas A, Watson AJ (2001) An investigation of frequency domain dispersion correction of pressure bar signals. Int J Impact Eng 25:87–101

Vaidya UK, Gautam ARS, Hosur M, Dutta P (2006) Experimental-numerical studies of transverse impact response of adhesively bonded lap joints in composite structures. Int J Adhes Adhes 26:184–198

Wang P, Xu LR (2006) Convex interfacial joints with least stress singularities in dissimilar materials. Mech Mater 38:1001–1011

Williams JG (1984) Fracture mechanics of polymers. Ellis Horwood, Chichester

Wu CML, Li RKY, Yeung LH (2003) Impact resistance of SM joints formed with ICA. J Electron Packag 125:93–97

Xu S, Dillard D (2003) Determining the impact resistance of electrically conductive adhesives using a falling wedge test. IEEE Trans Compon Packag Technol 26:554–562

Yokoyama T (2003) Experimental determination of impact tensile properties of adhesive butt joints with the split Hopkinson bar. J Strain Anal 38:233–245

Yokoyama T, Nakai K (2015) Determination of the impact tensile strength of structural adhesive butt joints with a modified split Hopkinson pressure bar. Int J Adhes Adhes 56:13–23

Yokoyama T, Shimizu H (1998) Evaluation of impact shear strength of adhesive joints with the split Hopkinson bar. JSME Int J Ser A 41:503–509

Yokoyama T, Nakai K, Mohd Yatim NH (2012a) High strain-rate compressive properties and constitutive modeling of bulk structural adhesives. J Adhes 88:471–486

Yokoyama T, Nakai K, Mohd Yatim NH (2012b) High strain-rate compressive behavior of bulk structural adhesives: epoxy and methacrylate adhesives. JSME Int J A-Solid M 6:131–143

Zhang F, Yang X, Xia Y, Zhou Q, Wang H-P, Yu T-X (2015) Experimental study of strain rate effects on the strength of adhesively bonded joints after hygrothermal exposure. Int J Adhes Adhes 56:3–12

Zhao H, Gary G (1996) On the use of SHPB techniques to determine the behaviour of materials in the range of small strains. Int J Solids Struct 33:3363–3375

Zwolinski M, Hickman J, Rubin H, Zaks Y, McCarthy S, Hanlon T, Arrowsmith P, Chaudhuri A, Hermansen R, Lau S, Napp D (1996) Electrically conductive adhesives for surface mount solder replacement. IEEE Trans Compon Packag Manuf Technol Part C 19:241–250